

Comb-locked cavity ring-down saturation spectroscopy


J. Wang, Y. R. Sun, L.-G. Tao, A.-W. Liu, T.-P. Hua, F. Meng, and S.-M. Hu

Citation: *Review of Scientific Instruments* **88**, 043108 (2017); doi: 10.1063/1.4980037

View online: <http://dx.doi.org/10.1063/1.4980037>

View Table of Contents: <http://aip.scitation.org/toc/rsi/88/4>

Published by the *American Institute of Physics*



Small Conferences. BIG Ideas.

Applied Physics
Reviews

SAVE THE DATE!
3D Bioprinting: Physical and Chemical Processes
May 2–3, 2017 • Winston Salem, NC, USA

The background of the banner features a blue-toned image of a human hand holding a glowing, branching structure that resembles a biological or chemical network, possibly representing a 3D bioprinted structure or a complex physical process.

Comb-locked cavity ring-down saturation spectroscopy

J. Wang,¹ Y. R. Sun,¹ L.-G. Tao,¹ A.-W. Liu,¹ T.-P. Hua,¹ F. Meng,² and S.-M. Hu¹

¹*Hefei National Laboratory for Physical Sciences at Microscale, iChem Center, University of Science and Technology of China, Hefei 230026, China*

²*National Institute of Metrology, Beijing 100013, China*

(Received 23 December 2016; accepted 29 March 2017; published online 17 April 2017)

We present a new method of comb-locked cavity ring-down spectroscopy for the Lamb-dip measurement of molecular ro-vibrational transitions. By locking both the probe laser frequency and a temperature-stabilized high-finesse cavity to an optical frequency comb, we realize saturation spectroscopy of molecules with kilohertz accuracy. The technique is demonstrated by recording the R(9) line in the $v = 3 - 0$ overtone band of CO near 1567 nm. The Lamb-dip spectrum of such a weak line (transition rate 0.0075 s^{-1}) is obtained using an input laser power of only 3 mW, and the position is determined to be 191 360 212 770 kHz with an uncertainty of 7 kHz ($\delta\nu/\nu \sim 3.5 \times 10^{-11}$), which is currently limited by our rubidium clock. *Published by AIP Publishing.* [<http://dx.doi.org/10.1063/1.4980037>]

I. INTRODUCTION

Precise frequencies of ro-vibrational transitions of molecules are of great interest in fundamental physics, for instance, verifying the stability of the proton-to-electron mass ratio¹ and searching parity violation effects in chiral molecules.^{2,3} They are also ideal optical frequency standards⁴⁻⁶ for their narrow natural widths, insensitive to stray magnetic fields, and spreading in a wide spectral region. Saturation spectroscopy is the most frequently used method to overcome the Doppler limit to derive precise line positions, but the strengths of molecular ro-vibrational transitions are usually very weak (transition rate is as low as a few mHz) and the saturation power is often too high to be reached by conventional tunable lasers. The difficulty can be circumvented by putting gas samples in an optical cavity with a very high finesse \mathcal{F} . It will drastically enhance the absorption path length with the factor \mathcal{F} , which can be $10^4 - 10^6$ by using a pair of commercially available high-reflective (HR) mirrors. Cavity-enhanced absorption techniques, including the widely used cavity ring-down spectroscopy (CRDS),⁷ have been applied to detect extremely weak molecular ro-vibrational transitions.^{8,9} At the same time, the light intensity inside the cavity is also considerably enhanced, which can significantly reduce the laser power needed for saturation spectroscopy.¹⁰⁻¹²

Spectral scan with sub-MHz precision can be realized by using a probe laser with its frequency locked to an external reference, like a stable etalon¹³ or an optical comb.¹⁴ However, the linewidth of the cavity mode is also reduced to be the free-spectral range (FSR) of the cavity divided by \mathcal{F} , as low as a few kHz. It is necessary to dynamically couple the probe laser beam into the cavity which has a very narrow linewidth, to overcome the drift of both the laser frequency and the cavity mode. A commonly applied method is to quickly sweep the cavity length to match the laser frequency.^{8,13-15} But the Doppler effect induced by the moving cavity mirror will reduce the frequency accuracy.^{14,16} Alternatively, one can sweep the probe laser frequency to match the cavity mode, while the cavity length can be locked on another frequency-stabilized

reference laser^{17,18} or even lock the probe laser to the cavity.¹⁹ In this case, the frequency accuracy is limited by both the probe laser and the reference laser (often a He-Ne laser). In the last decade, many molecular line positions in the mid-infrared have been determined from saturation spectroscopy using optical resonance cavities: SF₆,¹ CH₄,⁶ CO₂,^{11,20} HCOOH,²¹ and N₂O.²² In the near-infrared region, the Lamb-dip measurement has been limited to those relatively strong lines,^{12,23} which are mostly hydride molecules: C₂H₂,^{4,12,24-30} H₂O,^{31,32} and NH₃.³³ By measuring the narrow Lamb-dips with a width of below 1 MHz, these studies eliminated the uncertainty due to line profile models which must be considered for Doppler-limited studies^{14,30,34-38} and determined the line positions with kHz accuracy.

Here we present a new method of comb-locked cavity ring-down spectroscopy for the Lamb-dip measurement of molecular ro-vibrational transitions. The probe laser frequency and a temperature-stabilized high-finesse cavity are simultaneously locked with a fiber-based frequency comb. We demonstrate to use an input laser power of only 3 mW to record the Lamb-dip of a very weak overtone transition of CO near 1567 nm. The spectrometer can be applied to explore a large amount of molecular transitions in the infrared region with an accuracy of a few kHz.

II. EXPERIMENTAL SETUP

A diagram of the experimental setup is presented in Fig. 1. The main structure of the instrument includes two locking loops. One locks a narrow-band laser, which is used as the probe, to a temperature-stabilized ring-down (RD) cavity. The other one locks the ring-down cavity by using a frequency comb as the absolute reference and consequently lock the probe laser with the comb. The details of the setup are given below.

A fiber-amplified laser (NKT E15) with a stated linewidth of 1 kHz is used as the probe. It is locked to a longitudinal mode of the ring-down cavity using the Pound-Drever-Hall (PDH) method.³⁹ The resonance RD cavity is composed of two

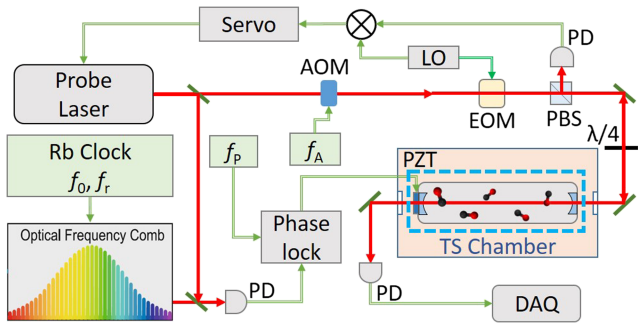


FIG. 1. Configuration of the experimental setup. AOM: acousto-optical modulator; DAQ: data acquisition system; EOM: electro-optical modulator; LO: local oscillator; PBS: polarizing beam splitter; PZT: piezo actuator; PD: photodiode detector; RF: radio frequency; TS: temperature-stabilized.

high-reflective mirrors setting apart with a distance of 44.6 cm, corresponding to a free-spectral range of 336 MHz. Each HR mirror has a reflectivity of 99.998% at 1.5–1.7 μm . Therefore, the RD cavity has a finesse of about 1.5×10^4 and a mode width of about 2.2 kHz. The PDH locking servo allows us to lock the probe laser frequency within about 1% of the cavity mode width. The RD cavity is made of aluminum, located in a stainless-steel vacuum chamber. An aluminum shield is used for thermal isolation between the RD cavity and the outer chamber. A feedback circuit controls the heating-current in a wire surrounding the aluminum shield to stabilize its temperature. Two platinum thermal sensors are attached at two sides of the RD cavity. The thermal sensors and the readout (Anton Parr, MKT50) were calibrated at the National Institute of Metrology (Beijing, China). The sensors show that the temperature of the RD cavity can be stabilized with a fluctuation below 1 mK for hours. As shown below, the thermal stability effectively reduces the frequency drift of the cavity modes.

An optical frequency comb operated at 1.57 μm is used as the absolute frequency reference. The comb is synthesized by an Er:fiber oscillator with its repetition frequency (f_r) and carrier offset frequency (f_0) referenced to a rubidium clock (Spectratime GPS Reference-2000). The beat signal between the probe laser and the frequency comb is phase-locked to a radio frequency (f_p), and the digital feedback servo drives a piezo actuator attached on one HR mirror to adjust the length of the RD cavity. We used a frequency counter (Agilent 53181A) to monitor the beat frequency between the probe laser and frequency comb, and the results are shown in Fig. 2. When the phase-lock loop is turned off and the RD cavity is free-run, the beat signal has a short-term fluctuation of about 0.1 MHz at 1 s and a long-term drift of about 1 MHz ($\Delta\nu/\nu \sim 5 \times 10^{-9}$) per hour. We think that the short-term fluctuation comes from the vibration noise on the RD cavity. The long-term frequency drift is consistent with the thermal expansion of the cavity under a temperature drift of 1 mK. When the phase-lock loop is turned on, the RD cavity length is stabilized. As a result, the probe laser frequency, which is locked to the cavity through the PDH locking servo, is eventually locked with the frequency comb. As shown in Fig. 2, the long-term drift of the probe laser frequency is eliminated. The short-term fluctuation also drastically decreases to less than 1 kHz ($\Delta\nu/\nu \sim 5 \times 10^{-12}$). It indicates that the vibration noise and thermal drift have been

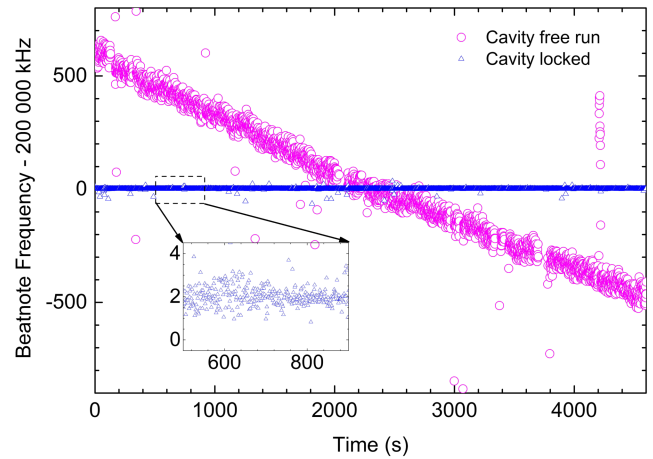


FIG. 2. Beatnote frequency between the probe laser and the frequency comb, when the ring-down cavity is locked (triangles) or set free (circles).

compensated and the residual fluctuation of about 1 kHz should come from the Rb clock which has a stated relative frequency stability of 1×10^{-11} at 1 s and an aging drift below 3×10^{-11} per month.

When the laser frequency is locked on the cavity, the power of the laser light emitted from the cavity, which is detected by a photodiode, reaches a steady level of about several tens of microwatts. It triggers an acousto-optical modulator (AOM) to block the probe laser beam to initiate a ring-down event. The signal is digitized and recorded by a fast digitizer installed in a personal computer. A fitting program based on the Levenberg-Marquardt algorithm is applied to fit the ring-down curve to an exponential decay function. The decay time τ is used to determine the absorption coefficient α of the sample in the RD cavity according to the equation,

$$\alpha(\nu) = \frac{1}{c\tau(\nu)} - \frac{1}{c\tau_0}, \quad (1)$$

where ν is the laser frequency, c is the speed of light, and τ_0 is the decay time of an empty cavity. During the period that the probe laser is blocked to record the ring-down signal, which lasts typically a few hundred microseconds, the PDH locking servo used to lock the probe laser frequency is temporarily turned off. When the RD-recording period finishes, the PDH locking servo is turned on again, the light field in the cavity is rebuilt, eventually the probe laser is locked on the cavity and the emitted laser power reaches the steady level again. Therefore, the locking-recording sequence repeats automatically. A sample of the recorded data, together with the schematic sequence of the locking control, is shown in Fig. 3. Note that the ring-down decay curve should be non-exponential when the absorption is saturated.^{11,40} For the sake of simplicity, we chose to fit the curve with a pure exponential function. The first reason is that the peak power in the cavity (will be discussed below) is still much less than the saturation power; therefore the RD curve is just slightly non-exponential. As shown in Fig. 3, the relative deviation is just at the 10^{-3} level. The second reason is that the main purpose of the present study is to derive precise line center frequencies instead of exact line profiles. The simplified exponential fit does not shift the center of the absorption line.

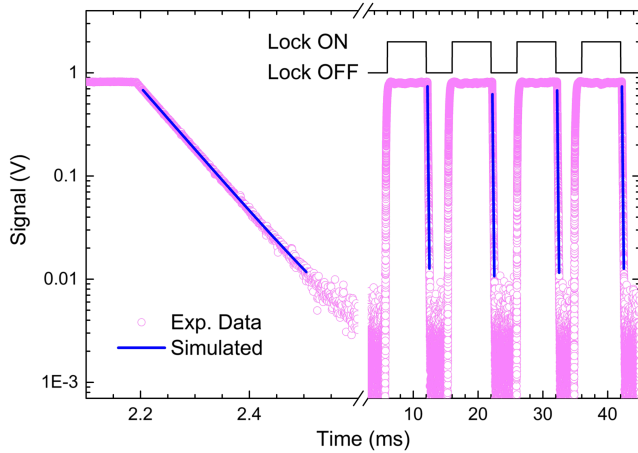


FIG. 3. The CRDS data with the probe laser frequency locked on the cavity. The open circles show the recorded signal and the solid line on the top of the circles is the simulated exponential decay curve. The corresponding locking control sequence is shown above the ring-down data.

In this way, the spectrum is recorded with a laser locked with kHz precision. The spectral scan is accomplished by tuning the reference frequency f_B of the phase-lock loop,

$$\nu = f_0 + nf_r + f_A + f_B, \quad (2)$$

where f_A is the radio frequency driving the AOM, and f_0 and f_r are the carrier offset frequency and repetition frequency of the comb, respectively. It is worth noting that the spectrometer can also work at the cavity enhanced absorption spectroscopy (CEAS) mode, by continuously detecting the transmitted light DC amplitude without blocking the probe laser.

For a resonant cavity composed of two identical HR mirrors, the cavity finesse \mathcal{F} , the cavity transmittance \mathcal{T} , and the cavity enhancement factor \mathcal{E} can be derived using the following equations:¹⁰

$$\mathcal{F} = \frac{\pi}{t + \ell + \alpha L}, \quad (3)$$

$$\mathcal{T} = \frac{P_t}{P_{in}} = \frac{t^2}{(t + \ell + \alpha L)^2}, \quad (4)$$

$$\mathcal{E} = \frac{P_c}{P_{in}} = \frac{P_c P_t}{P_t P_{in}} = \frac{\mathcal{T}}{t}, \quad (5)$$

where P_{in} , P_c , and P_t are the laser powers input to the cavity, inside the cavity, and transmitted from the cavity, respectively. t and ℓ are the transmittance and loss of single HR mirror, respectively, α is the sample absorption coefficient, and L is the cavity length. The reflectivity of the HR mirror, $r = 1 - t - \ell$, can be derived from the ring-down time of the empty cavity: $c\tau_0 \approx L/(1 - r)$. In our experiment, τ_0 is about 73 μ s, corresponding to a mirror reflectivity of $r = 0.99998$ and a finesse of 1.5×10^4 . We have also recorded the cavity transmittance spectrum using the probe laser, and we found that the width of the cavity mode is 2.3 kHz. It agrees well with the quotient of the FSR (336 MHz) and finesse of the cavity, $336\,000/15\,000 = 2.2$ kHz, indicating that the probe laser frequency jitter should be much smaller than the cavity width. We also measured a transmittance of 3% when the cavity is empty, and we got $t = 3.5 \times 10^{-6}$ and $\ell = 1.7 \times 10^{-5}$ according to Eq. (4). In this case, the power enhancement factor \mathcal{E} reaches about 8600 for an empty cavity.

III. RESULTS AND DISCUSSION

As a demonstration, the spectrometer was used to measure the saturation spectroscopy of the R(9) line in the $V = 3 - 0$ overtone band of $^{12}\text{C}^{16}\text{O}$. The transition located at 6383 cm^{-1} has a line intensity of $2.03 \times 10^{-23}\text{ cm/molecule}$ given in the HITRAN database.⁴¹ It has an Einstein coefficient of 0.0075 s^{-1} which corresponds to a saturation power of 30 W according to Ref. 11. We recorded the saturation spectrum of this line using a frequency step of 100 kHz. Each scan took about 70 s. A natural carbon monoxide sample was used and the sample pressure was 0.7 Pa. The central absorbance of the line at such sample pressure is $\alpha = 0.25 \times 10^{-6}\text{ cm}^{-1}$. An input laser power of 3 mW was used, and the laser power inside the cavity is estimated to be 11 W, according to Eq. (5), which is about 1/3 of the saturation power of the line.

Spectra were recorded with both CRDS and CEAS methods, and they are shown in Fig. 4. Since the probe laser is kept being locked on the RD cavity in the CEAS mode, the experimental implementation is simpler and the data acquisition is faster than that of CRDS. However, the signal-to-noise ratio in CEAS mode is lower than that in CRDS when the same time period is used in the measurement. As shown in Fig. 4, the signal-to-noise ratio in ring-down spectra is about 3 times higher than that in direct absorption spectra. The noise in the recorded spectra should be mainly from the fluctuation in the injected laser power, since the saturation effect depends on the total laser power built in the cavity. Because CRDS derives the absorption coefficient from the decay rate of the emitted light, it is less sensitive to the noise from laser power fluctuation.

Line parameters, including line center, width, and depth, can be derived from a fit of the spectrum. For simplicity, the Lorentzian function was used in the fit, which we found to be better than the Gaussian function. The linewidth is about 0.3 MHz (full width at half maximum), being consistent with a sum of the transit-time width (0.2 MHz) estimated from the laser beam waist (ϕ 0.7 mm) and the

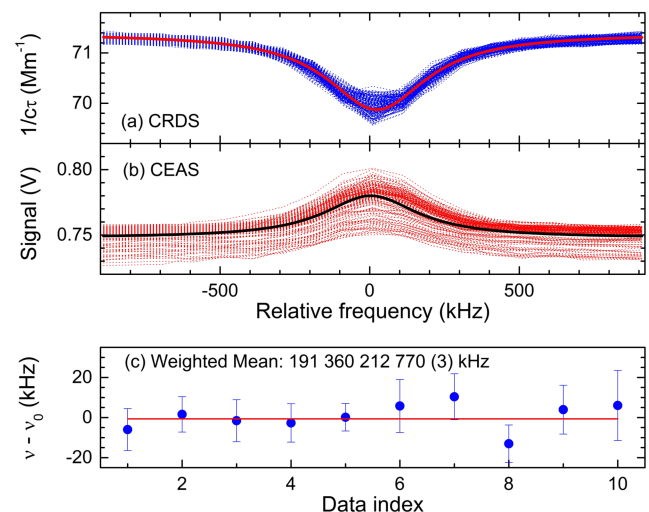


FIG. 4. Lamb-dip of the R(9) line in the 3-0 band of $^{12}\text{C}^{16}\text{O}$ measured by (a) cavity ring-down spectroscopy and (b) cavity enhanced absorption spectroscopy. (c) The line positions (error bar of statistical uncertainty) are obtained from different groups of data.

pressure-induced broadening (0.04 MHz).⁴² The observed depth of the Lamb-dip shown in Fig. 4 is about $2 \times 10^{-8} \text{ cm}^{-1}$, which is about one half of the value estimated according to the method given by Ma *et al.*¹⁰ A reason is that the static laser power inside the cavity (before the RD event occurs) was used in the estimation while the power is decreasing during the ring-down process. In addition, the simplified pure exponential function was used in the fit of the RD curve, while the decay of the intra-cavity power will reduce the saturation effect and lead to a non-exponential decay.¹¹ We notice that when we exclude more data points at the “tail” of the decay curve from the fit, we observed not only an increasing depth of the Lamb-dip but also an increasing noise level. In order to get an optimised sensitivity, only data in the initial 30 μs of each RD curve were included in the exponential fit to derive the absorption coefficient $\alpha(\nu)$.

Line positions derived from different groups of spectra (20 scans in each group) are shown at the bottom of Fig. 4. They agree with each other and give an averaged value of 191 360 212 770 kHz with a statistical uncertainty of 3 kHz. The self-induced line shift has been included, which is 1.3 kHz at 0.7 Pa according to the line shift coefficient of this line (-189 MHz/atm).⁴² We also recorded the spectrum using different intra-cavity laser power. However, within the present experimental uncertainty, we did not observe any power-dependent frequency shift for this CO line. The rubidium clock has a monthly fluctuation of about 3×10^{-11} , which leads to an uncertainty of 6 kHz in the absolute frequency. The radio frequency source (Rigol DG4062) and frequency counter (Agilent 53181A) are both referenced to the rubidium clock, and the uncertainties in f_B and f_A are below 0.5 kHz. The overall uncertainty of the determined line position is 7 kHz. The R(9) line position has previously been obtained from Doppler-limited spectra. Picqué and Guelachvili⁴² gave a position of 191 360 212.26 MHz with an uncertainty of 0.9 MHz from Fourier transform spectroscopy, and Mondelain *et al.*³⁶ gave 191 360 212.54 MHz with an uncertainty of 0.3 MHz from cavity ring-down spectroscopy. The present result is consistent with those values but the accuracy is improved by about two orders of magnitude.

As a summary, we introduce a new method of comb-locked cavity ring-down spectroscopy by locking both the probe laser frequency and the high-finesse cavity to an optical frequency comb. The frequency shift due to the instantaneous velocity of the cavity mirrors is eliminated, and the frequency precision is only limited by the linewidth of the probe laser and the frequency comb. It is worth noting that there is an increasing interest to perform sensitive cavity-enhanced detection using frequency combs as probing light sources.^{43,44} Such comb-based cavity ring-down (or cavity enhanced absorption) techniques take the advantage of broadband femtosecond laser sources which allows a fast acquisition of the spectrum over a broad spectral range, but the frequency accuracy is usually limited by Doppler-broadened line profiles. In this work, we use a frequency-locked cw laser for saturation spectroscopy and calibrate its absolute frequency with a frequency comb. It allows us to record Doppler-free absorption spectra with kilohertz accuracy. Since a huge amount of molecular transitions in the infrared can be measured in this way, it can

considerably improve the precision of line positions given in those widely used spectral databases including HITRAN.⁴¹ An upgrade of the present system, including using a more precise atomic clock standard, will allow us to improve the frequency accuracy to the sub-kHz level. Such a system would be applied in various studies such as the determination of physical constants⁴⁵ and the test of fundamental physics.²

ACKNOWLEDGMENTS

This work is jointly supported by CAS (No. XDB21020100), NBRPC (No. 2013CB834602), and NSFC (Nos. 21688102, 91436209, 21427804, and 21225314).

- ¹A. Shelkovich, R. J. Butcher, C. Chardonnet, and A. Amy-Klein, *Phys. Rev. Lett.* **100**, 150801 (2008).
- ²M. Quack, J. Stohner, and M. Willeke, “High-resolution spectroscopic studies and theory of parity violation in chiral molecules,” *Annu. Rev. Phys. Chem.* **59**, 741–769 (2008).
- ³S. K. Tokunaga, C. Stoefler, F. Auguste, A. Shelkovich, C. Daussy, A. Amy-Klein, C. Chardonnet, and B. Darquie, *Mol. Phys.* **111**, 2363 (2013).
- ⁴P. Balling, M. Fischer, P. Kubina, and R. Holzwarth, *Opt. Express* **13**, 9196 (2005).
- ⁵S. M. Foreman, A. Marian, J. Ye, E. A. Petrukhin, M. A. Gubin, O. D. Mücke, F. N. C. Wong, E. P. Ippen, and F. X. Kartner, *Opt. Lett.* **30**, 570 (2005).
- ⁶S. Okubo, H. Nakayama, K. Iwakuni, H. Inaba, and H. Sasada, *Opt. Express* **19**, 23878 (2011).
- ⁷A. Okeefe and D. A. G. Deacon, *Rev. Sci. Instrum.* **59**, 2544 (1988).
- ⁸S. Kassi and A. Campargue, *J. Chem. Phys.* **137**, 234201 (2012).
- ⁹Y. Tan, J. Wang, C.-F. Cheng, X.-Q. Zhao, A.-W. Liu, and S.-M. Hu, *J. Mol. Spectrosc.* **300**, 60 (2014).
- ¹⁰L. S. Ma, J. Ye, P. Dube, and J. L. Hall, *J. Opt. Soc. Am. B* **16**, 2255 (1999).
- ¹¹G. Giusfredi, S. Bartalini, S. Borri, P. Cancio, I. Galli, D. Mazzotti, and P. De Natale, *Phys. Rev. Lett.* **104**, 110801 (2010).
- ¹²D. Gatti, R. Gotti, A. Gambetta, M. Belmonte, G. Galzerano, P. Laporta, and M. Marangoni, *Sci. Rep.* **6**, 27183 (2016).
- ¹³H. Pan, C.-F. Cheng, Y. R. Sun, B. Gao, A.-W. Liu, and S.-M. Hu, *Rev. Sci. Instrum.* **82**, 103110 (2011).
- ¹⁴D. Gatti, T. Sala, R. Gotti, L. Coccola, L. Poletto, M. Prevedelli, P. Laporta, and M. Marangoni, *J. Chem. Phys.* **142**, 074201 (2015).
- ¹⁵C.-F. Cheng, Y. R. Sun, H. Pan, Y. Lu, X.-F. Li, J. Wang, A.-W. Liu, and S.-M. Hu, *Opt. Express* **20**, 9956 (2012).
- ¹⁶J. Y. Lee and J. W. Hahn, *Appl. Phys. B* **79**, 371 (2004).
- ¹⁷J. T. Hodges, H. P. Layer, W. W. Miller, and G. E. Scace, *Rev. Sci. Instrum.* **75**, 849 (2004).
- ¹⁸G. W. Truong, K. O. Douglass, S. E. Maxwell, R. D. van Zee, D. F. Plusquellic, J. T. Hodges, and D. A. Long, *Nat. Photonics* **7**, 532 (2013).
- ¹⁹A. Cygan, D. Lisak, P. Maslowski, K. Bielska, S. Wojtewicz, J. Domyslawska, R. S. Trawinski, R. Ciurylo, H. Abe, and J. T. Hodges, *Rev. Sci. Instrum.* **82**, 063107 (2011).
- ²⁰A. Amy-Klein, H. Vigue, and C. Chardonnet, *J. Mol. Spectrosc.* **228**, 206 (2004).
- ²¹F. Bielsa, K. Djerrou, A. Goncharov, A. Douillet, T. Valenzuela, C. Daussy, L. Hilico, and A. Amy-Klein, *J. Mol. Spectrosc.* **247**, 41 (2008).
- ²²W.-J. Ting, C.-H. Chang, S.-E. Chen, H.-C. Chen, J.-T. Shy, B. J. Drouin, and A. M. Daly, *J. Opt. Soc. Am. B* **31**, 1954 (2014).
- ²³J. Burkart, T. Sala, D. Romanini, M. Marangoni, A. Campargue, and S. Kassi, *J. Chem. Phys.* **142**, 191103 (2015).
- ²⁴F. L. Hong, A. Onae, J. Jiang, R. X. Guo, H. Inaba, K. Minoshima, T. R. Schibli, H. Matsumoto, and K. Nakagawa, *Opt. Lett.* **28**, 2324 (2003).
- ²⁵C. S. Edwards, H. S. Margolis, G. P. Barwood, S. N. Lea, P. Gill, and W. R. C. Rowley, *Appl. Phys. B* **80**, 977 (2005).
- ²⁶A. A. Madej, J. E. Bernard, A. J. Alcock, A. Czajkowski, and S. Chepurov, *J. Opt. Soc. Am. B* **23**, 741 (2006).
- ²⁷C. S. Edwards, G. P. Barwood, H. S. Margolis, P. Gill, and W. R. C. Rowley, *J. Mol. Spectrosc.* **234**, 143 (2005).
- ²⁸A. A. Madej, A. J. Alcock, A. Czajkowski, J. E. Bernard, and S. Chepurov, *J. Opt. Soc. Am. B* **23**, 2200 (2006).
- ²⁹S. Twagirayezu, M. J. Cich, T. J. Sears, C. P. McRaven, and G. E. Hall, *J. Mol. Spectrosc.* **316**, 64 (2015).

- ³⁰L. Santamaria, V. Di Sarno, P. De Natale, M. De Rosa, M. Inguscio, S. Mosca, I. Ricciardi, D. Calonico, F. Levi, and P. Maddaloni, *Phys. Chem. Chem. Phys.* **18**, 16715 (2016).
- ³¹D. Lisak and J. T. Hodges, *Appl. Phys. B* **88**, 317 (2007).
- ³²A. Gambetta, E. Fasci, A. Castrillo, M. Marangoni, G. Galzerano, G. Casa, P. Laporta, and L. Gianfrani, *New J. Phys.* **12**, 103006 (2010).
- ³³A. Czajkowski, A. J. Alcock, J. E. Bernard, A. A. Madej, M. Corrigan, and S. Chepurov, *Opt. Express* **17**, 9258 (2009).
- ³⁴D. A. Long, G. W. Truong, J. T. Hodges, and C. E. Miller, *J. Quant. Spectrosc. Radiat. Transfer* **130**, 112 (2013).
- ³⁵G. W. Truong, D. A. Long, A. Cygan, D. Lisak, R. D. van Zee, and J. T. Hodges, *J. Chem. Phys.* **138**, 094201 (2013).
- ³⁶D. Mondelain, T. Sala, S. Kassi, D. Romanini, M. Marangoni, and A. Campargue, *J. Quant. Spectrosc. Radiat. Transfer* **154**, 35 (2015).
- ³⁷M. Vainio and L. Halonen, *Phys. Chem. Chem. Phys.* **18**, 4266 (2016).
- ³⁸J. Peltola, M. Vainio, T. Fordell, T. Hieta, M. Merimaa, and L. Halonen, *Opt. Express* **22**, 32429 (2014).
- ³⁹R. W. P. Drever, J. L. Hall, F. V. Kowalski, J. Hough, G. M. Ford, A. J. Munley, and H. Ward, *Appl. Phys. B* **31**, 97 (1983).
- ⁴⁰P. Dupre, *Phys. Rev. A* **85**, 042503 (2012).
- ⁴¹L. S. Rothman, I. E. Gordon, Y. Babikov, A. Barbe, D. Chris Benner, P. F. Bernath, M. Birk, L. Bizzocchi, V. Boudon, L. R. Brown, A. Campargue, K. Chance, E. A. Cohen, L. H. Coudert, V. M. Devi, B. J. Drouin, A. Fayt, J. M. Flaud, R. R. Gamache, J. J. Harrison, J. M. Hartmann, C. Hill, J. T. Hodges, D. Jacquemart, A. Jolly, J. Lamouroux, R. J. Le Roy, G. Li, D. A. Long, O. M. Lyulin, C. J. Mackie, S. T. Massie, S. Mikhailenko, H. S. P. Müller, O. V. Naumenko, A. V. Nikitin, J. Orphal, V. Perevalov, A. Perrin, E. R. Polovtseva, C. Richard, M. A. H. Smith, E. Starikova, K. Sung, S. Tashkun, J. Tennyson, G. C. Toon, V. G. Tyuterev, and G. Wagner, *J. Quant. Spectrosc. Radiat. Transfer* **130**, 4 (2013).
- ⁴²N. Picqué and G. Guelachvili, *J. Mol. Spectrosc.* **185**, 244 (1997).
- ⁴³M. J. Thorpe, K. D. Moll, R. J. Jones, B. Safdi, and J. Ye, *Science* **311**, 1595 (2006).
- ⁴⁴A. J. Fleisher, D. A. Long, Z. D. Reed, J. T. Hodges, and D. F. Plusquellic, *Opt. Express* **24**, 010424 (2016).
- ⁴⁵Y. R. Sun, H. Pan, C.-F. Cheng, A.-W. Liu, J.-T. Zhang, and S.-M. Hu, *Opt. Express* **19**, 19993 (2011).